Geometric and Electronic Structure of Co(II)-Substituted Azurin

Jan O. A. De Kerpel and Kristine Pierloot*

Department of Chemistry, University of Leuven, Celestijnenlaan 200F, B-3001 Heverlee-Leuven, Belgium

Ulf Ryde

Department of Theoretical Chemistry, Lund University, Chemical Centre, P.O. Box 124, S-221 00 Lund, Sweden

Received: April 26, 1999; In Final Form: July 8, 1999

The molecular and electronic structures of Co(II)-substituted azurin have been investigated using several realistic models of the metal coordination sphere. The geometry of the models was optimized using the hybrid density functional B3LYP method and compared to the structures obtained for similar Cu(II) models. It is found that Co(II) prefers a distorted tetrahedral structure with four strong bonds to two histidine nitrogens, the cysteine sulphur, and the backbone carbonyl group. This is in contrast to Cu(II), where two weak axial bonds to methionine and the backbone oxygen are found, combined with three strong bonds to the histidines and cysteine in the equatorial plane of a trigonal bipyramidal structure. The optimal structure of the models conforms with experimental crystal data, indicating that the active-site structure in these proteins is determined by the preferences of the metal ion and its ligand and not by protein strain. The electronic structure and spectrum of the $Co(imidazole)_2(SH)(SH)_2(HCONH_2)^+$ model have been investigated in detail using multiconfigurational second-order perturbation theory based on a complete active-space wavefunction (CASPT2). Nine ligand-field transitions and six $S_{cys} \rightarrow Co$ charge-transfer transitions have been calculated, and all experimentally observed absorption bands in the absorption spectrum of Co(II) azurin have been assigned. It is shown that the $Co-S_{cys}$ bond is more ionic than the $Cu-S_{cys}$ bond and that this causes the blue shift and weakening of the charge-transfer states in the spectrum of Co(II)-substituted azurin compared to native copper protein.

1 Introduction

Azurins are small blue copper proteins (less than 130 amino acid residues) containing a type 1 copper site.[1,2] The copper ion is strongly bound to a cysteine S^γ atom and to the N^δ atoms of two histidine residues. It is situated slightly above the plane formed by these three strongly ligating atoms (∼10 pm) toward a weakly interacting methionine S^δ atom. Furthermore,a weak interaction is also observed with a backbone carbonyl oxygen atom. The azurin site is therefore often described as distorted trigonal bipyramidal. All other blue copper proteins show a similar copper coordination except for the carbonyl oxygen coordination, which is unique for the azurins. In the other blue copper proteins, the Cu−O distance is considerably larger, 380−600 pm.

All blue copper proteins exhibit three features that differ from what is found for small inorganic copper complexes: a strong absorption around 600 nm (ϵ in the range of 3000 to 7000 M^{-1} cm^{-1}) together with a second absorption of varying intensity at 460 nm, anomalously small hyperfine coupling constants in the electron spin resonance spectrum, and a high reduction potential. It has been shown that the strong bond between S_{cys} and copper is essential for these properties, while the axial ligands are of minor importance for the electronic characteristics of the active site.[3−6] For example, in stellacyanin the methionine ligand is replaced by a glutamine amide oxygen, but still it exhibits all of the blue copper characteristics. It has also been shown that in the azurins, the backbone carbonyl oxygen is barely interacting with the copper ion.[7]

Paramagnetic NMR spectroscopy has been shown to be a powerful tool for investigating the coordination environment of the Cu(II) active sites. However, paramagnetic NMR peaks of Cu(II) species are not as readily assigned as those of analogous Co(II) and Ni(II) proteins.[8] Many features of the copper coordination environment of structurally undetermined proteins and mutants have therefore been interpreted based on the NMR results for metal-substituted proteins.[9,10] Of course, this is only reasonable if one may assume that the metal substitution has little effect on the active-site geometry.[11] Crystal structures and NMR spectroscopy have indicated that the carbonyl oxygen binds much more strongly in the cobalt- and nickel-substituted azurins (210−240 pm) than in the native protein. Simultaneously, the metal$-S_{met}$ distance increases to about 330−350 pm.[12,13] Thus, these metal-substituted azurin sites adopt a distorted tetrahedral geometry where the metal has moved in the direction of the backbone carbonyl oxygen and away from the methionine residue.

In a series of papers[4,5,14−17] we have presented a thorough theoretical investigation of the molecular and electronic structure of different blue copper proteins. The series started with the observation[14] that the extraordinary trigonal structure of axial type 1 copper proteins in their oxidized form is not imposed by the tertiary protein structure, as was originally suggested in the entatic state and induced-rack theories,[18,19] but is instead the preferred geometry of a Cu(II) ion with the ligand set presented

* Corresponding author fax: +32-16 32 79 92; e-mail: kristin.pierloot@chem.kuleuven.ac.be.

10.1021/jp991359g CCC: $18.00
Published on Web 09/09/1999

by the protein. Further studies pointed to the importance of the $Cu-S_{cys}$ bond, both for the molecular structure[16] and for the characteristics of the electronic spectra of blue copper proteins.[4,5,15] Different proteins, e.g., plastocyanin, cucumber basic protein, pseudoazurin, nitrite reductase, and stellacyanin, were examined, and a relation was established between the subtle structural differences between these proteins and the much more striking differences in their electronic spectra.

In this paper we extend our investigation to a metal-substituted blue copper protein, viz. azurin, in which the Cu(II) ion has been replaced by Co(II), a transition metal ion with its own structural preferences. We examine to what extent this ion is capable of manipulating the original Cu(II) environment to reach its own optimum coordination geometry. We also investigate the electronic spectrum of this protein and relate the differences observed in the spectra of the two ions to their different ground-state electronic structure.

2 Methods

2.1 Geometry Optimizations. The geometry of the active site of Co−azurin has been modeled with the same ligands as used in our previous studies of other blue copper proteins.[4,5,14,15] The histidine ligands are modeled by imidazole (Im), the cysteine residue by $S(CH_3)_2$, and the backbone amide group by $CH_3CONH(CH_2)_2Im$, a model that includes the link to the neighboring histidine ligand in the same way as in the protein. No symmetry constraints were employed in the optimizations.

The model complexes were optimized using the hybrid density functional method B3LYP as implemented in the Turbomole[20] software. The 6-31G* basis sets were used for all atoms, except for cobalt and copper where we used the double-ζ basis of Schäfer et al.,[21] enhanced with *p*, *d*, and *f* functions with exponents 0.174, 0.132, and 0.39, or 0.141308, 0.043402 (two *p* functions), 0.1357, and 1.62, respectively. Only the pure five *d* and seven *f*-type functions were used.

Throughout the discussion, a coordinate system is defined in the following way: the copper ion is at the origin, the *z* axis is along the $Cu-S_{met}$ bond, and the $Cu-S_{cys}$ bond is situated in the *xz* plane.

2.2 Spectral Calculations. Calculations of the electronic spectra were performed using the CASSCF/CASPT2 approach (second order perturbation theory with a multiconfigurational reference state).[22] The calculations were performed on the $Co(Im)_2(SH)(SH_2)(HCONH_2)^+$ model optimized with the B3LYP method in C_s symmetry. This symmetry restraint is necessary for technical reasons, but it also facilitates the characterization of the various excitations. Moreover, the restraint has a small influence on the geometry of the complex, as can be seen in Table 2. Only the very flexible $Co-S_{met}$ bond is significantly changed (it is shorten by 25 pm), but it is still very weakly interacting with the metal ion. The CASSCF active space consisted of 11 electrons distributed in 12 orbitals, chosen as follows: five Co 3d orbitals, five correlating Co 3d′ orbitals, and two S_{cys} 3p orbitals. With this active space, it is possible to describe the seven ^4F and three ^4P Co(II) ion terms and the six charge-transfer states resulting from the transitions of two S_{cys} 3p orbitals into the three singly occupied Co 3d orbitals. For all states belonging to a given symmetry (A′ or A″), a state average CASSCF wavefunction was calculated for each multiplet and each symmetry. Thus, separate calculations are performed for the three or four ^4F states of symmetry A′ and A″, respectively, and for the two ^4P states of symmetry A″. The single ^4P ligand-field state of symmetry A′ was calculated by a single-root CASSCF calculation. The state-average calculations of the charge-transfer states included also the ^4P states of the respective symmetry representation (to avoid root flipping between the charge-transfer and the ^4P states). The state-average CASSCF calculations were followed by a CASPT2 calculation on each individual state. In the CASPT2 calculations all electrons originating from Co 3s,3p,3d; S 3s,3p; C,N,O 2s,2p; and H 1s were correlated.

The basis sets used in the CASSCF/CASPT2 calculations were of the generally contracted atomic natural orbital (ANO) type,[23] contracted in the following way: Co [17s12p9d4f/6s4p3d1f], S [13s10p4d/4s3p1d], O [10s6p3d/3s2p1d], N and C [10s6p/3s2p], H [7s/2s] for hydrogens bound to sulphur atoms, and [7s/1s] for hydrogens bound to imidazole and formamide. Previous work has shown that these moderate-size contractions are sufficient to give a proper description of the spectra of blue copper proteins.[4]

Relativistic corrections (Darwin and mass-velocity), calculated at the CASSCF level, were added to the CASPT2 excitation energies. A level-shift, added to the zeroth order Hamiltonian, was used to remove intruder states. It has been shown that a level-shift of 0.3 a.u. is appropriate to remove all intruder states without deteriorating the excitation energies.[24] This value was also used successfully for the present systems. Oscillator strengths were obtained from transition dipole moments computed with the CAS state-interaction method[25] at the CASSCF level in combination with CASPT2 excitation energies. Even though the results obtained for the oscillator strengths should be considered as qualitative, they are useful as a measure for the relative intensity of the different transitions.

The CASSCF/CASPT2 calculations were performed with the MOLCAS-4 quantum chemistry software[26] and all calculations were run on IBM RS/6000 workstations.

3 Results and Discussion

3.1 The Active-Site Geometry of Co(II)-Substituted Azurin. Azurins from many bacteria, e.g., *Pseudomonas aeruginosa*, are tetramers of four identical subunits. In Table 1, the geometry of the four active-site metal ions of both wild-type and Co-substituted *P. aeruginosa* azurin is described.[13,27] All Co-ligand distances are longer than the corresponding Cu-ligand distances, except for the distance to the backbone oxygen ligand, which is 75 pm shorter. This change is accomplished by a movement of the metal ion: the copper ion is found about 25 pm below this plane, in the direction of the oxygen atom. The overall geometry of the active sites is slightly changed: the copper active site can be described as trigonal bipyramidal with two long bonds to the axial ligands, whereas the cobalt active site is distorted tetrahedral, due to the short Co−O distance and the virtual absence of a $Co-S_{met}$ bond.

We have optimized the geometry of several realistic models of the azurin active site with either a copper or a cobalt ion. Such calculations are complicated by the fact that the axial ligands often interact very weakly with the metal ion.[28] Therefore, we first optimized structures with only one axial ligand. In Table 2, the geometry of $Cu/Co(Im)(Im(CH_2)_2NHCOCH_3)(SCH_3)^+$ is shown. These complexes include a realistic model of the backbone amide ligand ($CH_3CONHCH_2-$) which is connected to the histidine imidazole ring in the same way as in the protein (by a CH_2 bridge). It can be seen that the Co−O bond is 26 pm shorter than the Cu−O bond (207 compared to 234 pm), whereas the $Co-S_{cys}$ bond is 5 pm longer than the $Cu-S_{cys}$ bond (222 compared to 217 pm). This difference is mainly due to the fact that the copper structure is trigonal with a π bond between copper and S_{cys}. The corre-

TABLE 1: Distances (pm) and Angles (deg) around the Active-Site Metal Ions in the Four Subunits of Native and Cobalt-Substituted Azurin from *P. aeruginosa*[a]

	Co active sites					Cu active sites				
	A	B	C	D	av	A	B	C	D	av
distances (pm)										
S_{cys}	235	231	236	233	234	227	227	224	217	224
O_{gly}	214	232	225	221	223	284	295	305	303	297
S_{met}	358	340	370	356	356	318	316	321	305	315
N_{his46}	237	231	247	254	242	211	206	213	212	211
N_{his117}	226	228	218	226	225	200	198	196	200	199
angles (deg)										
$O_{gly}-S_{cys}$	105	103	104	104	104	99	100	96	101	99
$O_{gly}-S_{met}$	148	147	151	150	149	149	145	150	148	148
$O_{gly}-N_{his46}$	79	73	84	80	79	77	74	77	68	74
$O_{gly}-N_{his117}$	93	107	101	103	101	90	91	87	88	89
$S_{cys}-S_{met}$	96	105	101	96	100	110	111	111	108	110
$S_{cys}-N_{his46}$	120	128	134	119	125	132	128	136	131	132
$S_{cys}-N_{his117}$	122	123	117	123	121	124	124	118	124	123
$S_{met}-N_{his46}$	69	75	68	70	71	75	74	75	82	77
$S_{met}-N_{his117}$	96	73	79	83	83	84	86	90	88	87
$N_{his46}-N_{his117}$	117	107	105	115	111	104	108	105	104	105

[a] The data are taken from the pdb files 1vlx and 4azu.[13,27]

TABLE 2: Distances (pm) and Angles (deg) of the Various Copper and Cobalt Models of the Active Site of Azurin

	Distances to Co			
	S_{met}	O	S_{cys}	N
$Co(Im)_2(SH)(SH_2)(HCONH_2)^+$ [a]	414	208	224	206
$Co(Im)_2(SH)(SH_2)(HCONH_2)^+$	439	209	223	204−205
$Co(Im)(Im(CH_2)_2NHCOCH_3)(SCH_3)^+$		207	222	206−208
$Cu(Im)(Im(CH_2)_2NHCOCH_3)(SCH_3)^+$		233	217	202−206
$Cu(Im)(Im(CH_2)_2NHCOCH_3)(SCH_3)^+$ [b]		216	226	201−203
$Co(Im)_2(SCH_3)(S(CH_3)_2)^+$	243		222	206−207
$Cu(Im)_2(SCH_3)(S(CH_3)_2)^+$	267		218	204
$Cu(Im)_2(SH)(S(CH_3)_2)^+$ [b]	242		223	205−206
$Co(Im)(Im(CH_2)_2NHCOCH_3)(SCH_3)(S(CH_3)_2)^+$ [c]	719	208	223	206
$Co(Im)(Im(CH_2)_2NHCOCH_3)(SCH_3)(S(CH_3)_2)^+$ [d]	356	212	222	206−209
$Co(Im)(Im(CH_2)_2NHCOCH_3)(SCH_3)(S(CH_3)_2)^+$ [e]	356	223	222	206−208
$Cu(Im)(Im(CH_2)_2NHCOCH_3)(SCH_3)(S(CH_3)_2)^+$ [c]	718	234	217	203−204
$Cu(Im)(Im(CH_2)_2NHCOCH_3)(SCH_3)(S(CH_3)_2)^+$ [e]	312	316	217	202
crystal structure, average	356	223	234	227−239

	Angle Subtended at Co						
	$S_{met}-S_{cys}$	$S_{met}-N$	$S_{met}-O$	$O-S_{cys}$	O−N	$S_{cys}-N$	N−N
$Co(Im)_2(SH)(SH_2)(HCONH_2)^+$ [a]	96	69−96	148	105	79−93	120−122	117
$Co(Im)_2(SH)(SH_2)(HCONH_2)^+$	84	67−84	169	103	101−100	116−119	114
$Co(Im)(Im(CH_2)_2NHCOCH_3)(SCH_3)^+$				114	95−97	117−120	109
$Cu(Im)(Im(CH_2)_2NHCOCH_3)(SCH_3)^+$				109	88−91	126−127	102
$Cu(Im)(Im(CH_2)_2NHCOCH_3)(SCH_3)^+$ [b]				134	90−105	96−101	138
$Co(Im)_2(SCH_3)(S(CH_3)_2)^+$	117	104−108				102−117	109
$Co(Im)_2(SCH_3)(S(CH_3)_2)^+$	117	94−95				119−123	103
$Co(Im)_2(SH)(S(CH_3)_2)^+$ [b]	103	95−126				98−141	100
$Cu(Im)(Im(CH_2)_2NHCOCH_3)(SCH_3)(S(CH_3)_2)^+$ [c]				111	96	116−121	112
$Cu(Im)(Im(CH_2)_2NHCOCH_3)(SCH_3)(S(CH_3)_2)^+$ [d]	97	71−86	156	103	91−92	116−128	114
$Cu(Im)(Im(CH_2)_2NHCOCH_3)(SCH_3)(S(CH_3)_2)^+$ [e]	96	70−86	160	103	91−93	115−129	113
$Cu(Im)(Im(CH_2)_2NHCOCH_3)(SCH_3)(S(CH_3)_2)^+$ [c]				106	90−91	121−133	103
$Cu(Im)(Im(CH_2)_2NHCOCH_3)(SCH_3)(S(CH_3)_2)^+$ [e]	107	82−91	149	103	72−80	124−131	103
crystal structure, average	96	69−96	148	105	79−93	120−122	117

[a] Enforced to have C_s symmetry (all the other complexes involve no symmetry restraints). [b] A tetragonal structure (with σ bonds to the four close ligands; all the other Cu structures are trigonal (with a $Cu-S_{cys}$ π bond). [c] The methionine model is effectively dissociated, being hydrogen-bonded to the noncoordinating nitrogen atom of an imidazole group. [d] The $Co-S_{met}$ distance has been constrained to the crystal value. [e] The metal$-S_{met}$ and metal−O distances have been constrained to their crystal values.

sponding tetragonal copper structure (with σ bonds to all four ligands, as in the cobalt complex), is also shown in Table 2 and it has a 7 pm shorter Cu−O bond and a 9 pm longer Cu−S_{cys} bond, which makes the metal-ligand distances quite similar to those of the cobalt structure. Quite naturally, the copper structure is closely similar to the optimized structure of a model of the active site of stallacyanin (which has the same ligands, but no link between imidazole and the amide group), except for a 10 pm longer Cu−O bond in the present structure.[15] The latter difference is most likely due to steric restrictions introduced by the link, in combination with a flat potential surface (see below).

The structures of $Cu/Co(Im)_2(SCH_3)(S(CH_3)_2)^+$ are also shown in Table 2. They include a methionine model ($S(CH_3)_2$) but no amide group. Again, the copper structure has a shorter bond to S_{cys} and a longer bond to the axial ligand, but in this case the $Co/Cu-S_{met}$ bonds are quite long, 243−267 pm. In the table, the tetragonal structure (i.e., a complex with four

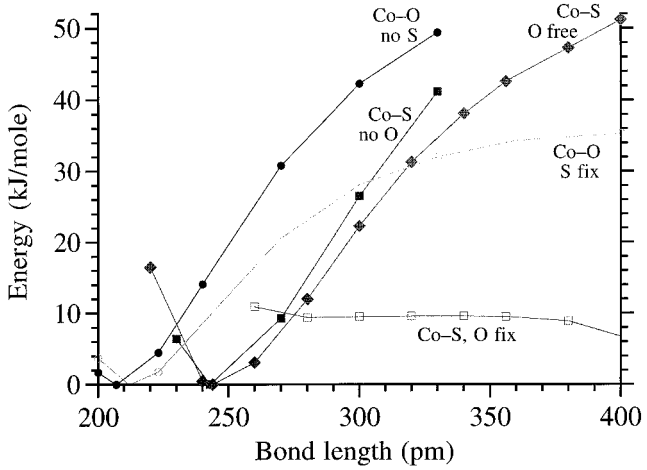

Figure 1. Potential surfaces of the Co−S_{met} and Co−O bonds in various model systems. Here, "no S" and "no O" denote the Co(Im)-$(Im(CH_2)_2NHCOCH_3)(SCH_3)^+$ and $Co(Im)_2(SCH_3)(S(CH_3)_2)^+$ complexes, respectively, whereas the other three lines have been obtained using the $Co(Im)(Im(CH_2)_2NHCOCH_3)(SCH_3)(S(CH_3)_2)^+$ model with the Co−O or Co−S_{met} distances either free or fixed to their crystal values, 223 or 356 pm, respectively.[13]

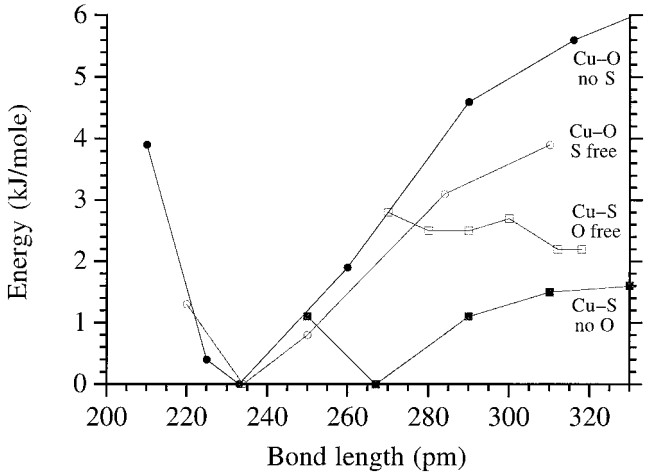

Figure 2. Potential surfaces of the Cu−S_{met} and Cu−O bonds in various model systems. Here, "no S" and "no O" denote the Cu(Im)-$(Im(CH_2)_2NHCOCH_3)(SCH_3)^+$ and $Cu(Im)_2(SCH_3)(S(CH_3)_2)^+$ complexes, respectively, whereas the other two lines have been obtained using the $Cu(Im)(Im(CH_2)_2NHCOCH_3)(SCH_3)(S(CH_3)_2)^+$ model with the Co−O or Co−S_{met} distances at their equilibrium distances.

σ-bonds, as in the Co structure) of a slightly smaller copper complex is also included $(Cu(Im)_2(SH)(S(CH_3)_2)^+$; a tetragonal structure cannot be found with the larger complex). It can be seen that the metal-ligand bond lengths of this complex are very similar to those of the cobalt complex. Thus, the differences in the metal-ligand bond lengths between the trigonal copper complex and the cobalt complex are mainly due to the electronic structure of the copper complex (the π bond between Cu and S_{cys}).

Finally, we optimized structures of complexes with both axial ligands (e.g., $Co(Im)(Im(CH_2)_2NHCOCH_3)(SCH_3)(S(CH_3)_2)^+$). For both metals, the most stable structure of these complexes is very similar to the one of complexes without the methionine model, since the methionine group tends to dissociate from the metal ion and to bind instead by a hydrogen bond to $H^{\epsilon 2}$ of one of the imidazole groups. This implies that the interaction between the methionine group and the metal ion is weaker than this hydrogen bond.

In order to obtain geometries that can be compared to the crystal structure, we reoptimized the structure of the above model with the Co−O and Co−S_{met} distances constrained to the average crystal values, 223 and 356 pm. Such a structure is 30 kJ/mole less stable than the optimum structure. The rather large energy difference is mainly due to the hydrogen bond between imidazole and S_{met}, which gives about 37 kJ/mole (including corrections to the basis set superposition error) in the optimized complex. In the protein, other groups may form hydrogen bonds to S_{met} and the imidazole group, so this hydrogen bond energy is not relevant for the energetics of the cobalt complexes.

Therefore, we followed the potential surfaces of the Co−S_{met} and Co−O bonds. The results are shown in Figure 1. It can be seen that in four-coordinate complexes, no matter if the fourth ligand is the amide or methionine groups, the potential surfaces are quite normal; the harmonic force constant for the Co−O bond around the minimum is about 0.023 kJ/mole/pm^2 (i.e., it costs about 10 kJ/mole to change the Co−O distance 20 pm from the optimum value). Similarly, the harmonic force constant for the Co−S_{met} bond is 0.021 kJ/mole/pm^2. The Co−O potential curve does not change mucb if a methionine model is added at the crystal distance (356 pm; the harmonic force constant is 0.021 kJ/mole/pm^2). Neither does the Co−S_{met} potential curve change if an amide model is added at a rather large distance (there is a second local minimum for this group at a Co−O distance of 420−470 pm; the harmonic force constant is 0.016 kJ/mole/pm^2). However, if the amide ligand is fixed at the crystal distance, things change radically: Then, the Co−S_{met} potential surface becomes extremely flat, so flat that the Co−S_{met} bond length can be changed between 280 and 380 pm at a cost of less than 1 kJ/mole.

These results directly explain the crystal structure of Co−azurin. The Co−O distance is close to its optimum value (207−212 pm in the optimizations) and the amide group is a true ligand of cobalt. The methionine group is very weakly associated to the metal site and its position is not determined by the metal but by surrounding groups presenting hydrogen donors and acceptors, and probably also by nonpolar interactions. The flat Co−S_{met} potential surface also explains the large variation of this bond length among the four subunits in the crystal structure (340−370 pm).

The behavior of the cobalt complex is in sharpn contrast to that of the copper site. As can be seen in Figure 2, the potential surfaces of both the Cu−O and Cu−S_{met} bonds are very flat, no matter if the site is four- or five-coordinate. Thus, the Cu−O harmonic force constant is 0.005 kJ/mole/pm^2 around the minimum, and the Cu−S_{met} force constant is 0.003 kJ/mole/pm^2, i.e., four to eight times smaller than the corresponding constants for the cobalt complexes. Therefore, it costs only about 6 kJ/mole to change the Cu−azurin models from their optimum geometry to a structure with the two axial ligands fixed at their crystal distances. Such an energy is within the error limits of the quantum chemical method, so we can not with certainty decide the actual optimum structure of the copper complexes.

However, these results clearly explain the difference between the structure of cobalt and copper azurin. The cobalt site is four-coordinate with a strong bond to the amide group. Therefore, the energy to move this group from the distance observed in the native protein (about 300 pm) to the optimum distance (207−212 pm) is so high (30−40 kJ/mole) that the protein cannot obstruct such a movement. For copper, on the other hand, the site is effectively three-coordinate with two weak axial ligands (due to the trigonal, π bonded, electronic structure). The force constants for the interaction between these two ligands

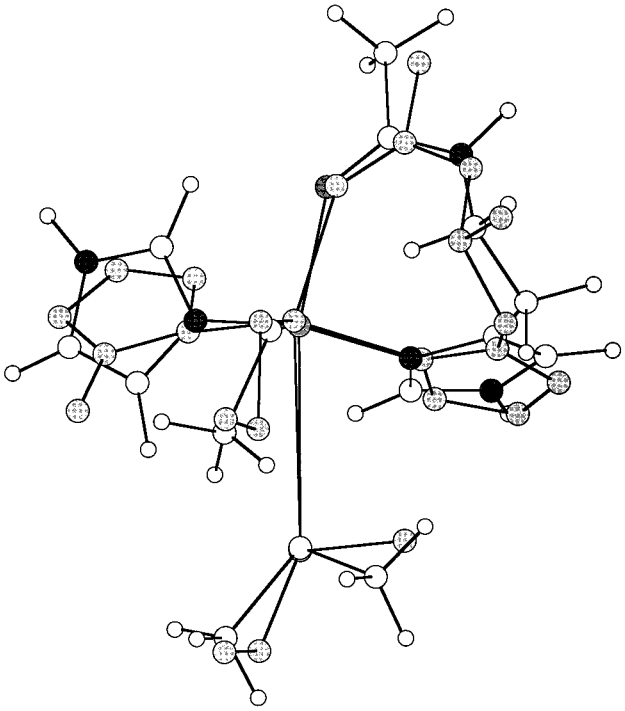

Figure 3. A comparison between the crystal structure of Co−azurin (shaded)[13] and the $Co(Im)(Im(CH_2)_2NHCOCH_3)(SCH_3)(S(CH_3)_2)^+$ model, optimized with the $Co-S_{met}$ bond length constrained at the crystal value (356 pm).

and the copper ion are so small that the protein may modulate these bonds by electrostatics and other interactions. At present, it is not possible to decide the preferred geometry of this site, but it is clear that it is not distorted by more than 6 kJ/mole in the protein. It should be noted that the energies involved are so small that they can hardly be called protein strain. Instead, they reflect that the methionine ligand is barely bound to the metal ion in vacuum. Therefore, it adapts to any interactions presented by the protein. The copper site will be more thoroughly investigated in a forthcoming publication.[28]

In Figure 3, the crystal structure of Co−azurin is compared to the $Co(Im)(Im(CH_2)_2NHCOCH_3)(SCH_3)(S(CH_3)_2)^+$ model, optimized with the $Co-S_{met}$ bond length constrained to the crystal value. Clearly, the general structure of the optimized complexes is quite similar to the protein structure. From Table 2, it can be seen that all angles around the Co ion fall well inside the range observed in the crystal structure, except the $O-Co-S_{met}$ angle, which is slightly larger in the optimized structure (156° compared to 147−151° in the crystal structure), probably because the methionine ligand interacts so weakly with the metal ion in the protein. However, for the Co−ligand distances, some larger deviations can be seen. The Co−O bond is 11 pm shorter and the $Co-S_{cys}$ distance is 12 pm longer in the optimized structure than in the averaged crystal structure. These differences are within the uncertainty of the crystal structure and they are probably insignificant, especially considering that the average distances published in the paper about Co−azurin[13] are much closer to ours (215 pm for Co−O and 220 pm for $Co-S_{cys}$; the distances in Tables 1 and 2 are taken from the PDB file, 1vlx).

However, for the Co−N distances, the difference is larger, 17−26 pm, which may seem to be somewhat too large to be caused by the experimental uncertainty. Therefore, we have thoroughly tried to find local minima on the potential energy surface that could account for the observed longer Co−N distances, but all such attempts have given structures with short Co−N bonds. We have also optimized a structure of $Co(Im)_2(SH)(HCONH_2)^+$ with the Co−N bond lengths constrained to the crystal values. Such a structure is 52 kJ/mole less stable than the optimum structure (with short Co−N bonds). Considering that we have estimated that the maximum distortion energies in the blue copper proteins are around 10−20 kJ/mole,[29] it seems unlikely that azurin could distort the ligand sphere by such a large energy. Moreover, there is no reason why azurin should affect only the cobalt structure and not the native copper structure, which has much shorter Cu−N bonds (196−213 pm). It should be noted that our optimized copper models have Cu−N distances of 202−206 pm, well inside this range.

Furthermore, Bonander et al.[13] have searched the Cambridge Data Base for small transition-metal structures with at least a NNS metal coordination (no cobalt complex was found with the same coordinating atoms as in azurin). The 28 studied structures were either tetragonal or trigonal and showed the following ranges for the Co-ligand distances: Co−S: 223−246 pm; Co−O: 190−216 pm; and Co−N: 195−214 pm. The $Co-S_{cys}$ and Co−O distances in the crystal structure of Co−azurin are within these ranges, as are the distances obtained in our optimized structures. However, the experimental values of the Co−N distance (225−232 pm) are 11−18 pm longer than the maximum Co−N value in the database, whereas our calculated values lie within the database range. It should also be noted that all optimized Cu−N bond lengths in our previous investigations of blue copper proteins (e.g., plastocyanin, stellacyanin, and nitrite reductase),[5,14,15] 202−206 pm, lie well in the range observed for copper complexes in a similar search of the Cambridge Data Base, 193−226 pm.[13] Together, all of these results lead us to suggest that observed Co−N distances in the crystal structure (which has a resolution of 190 pm) are about 20 pm too long.

In conclusion, our quantum chemical calculations give an excellent description of the structure of Co−azurin. In fact, they probably give a higher accuracy around the metal site than crystal structures at the resolution normally obtained for proteins (150−300 pm). The calculations explain why the backbone oxygen ligand binds at a short distance to cobalt but not to copper. This is an effect of the electronic structure of the copper complex (the π-bond between Cu and S_{cys}; see also next section). Moreover, our results once again[30] show that the structure of the blue copper proteins is determined by the preferences of the metal ion and its ligands, and not by protein strain. More quantitatively, they show that azurin cannot produce strain energies of 30−40 kJ/mole. In fact, from the observed experimental and optimized lengths of the Co−O bond, we can calculate a maximum strain energy for this bond of only 2 kJ/mole. However, we also observe that the protein may modulate the position of the weakly bound methionine ligand. Yet, the involved energies are low, less than 3 kJ/mole, and they originate from interactions that normally are not considered as mechanical strain, viz. hydrogen bonds and hydrophobic forces.

3.2 The Electronic Spectrum of Cobalt Azurin. In order to explain the electronic spectrum of Co(II)-substituted azurin, a series of CASSCF/CASPT2 calculations were performed on the symmetric $Co(Im)_2(SH)(SH_2)(HCONH_2)^+$ model optimized with the B3LYP method (c.f. Table 2). The results of these calculations are shown in Table 3, and they are compared to our previous results obtained for a model of plastocyanin ($Cu(Im)_2(SH)(SH_2)^+$) in Table 4.[4] The latter complex lacks a model of the axial backbone oxygen ligand in azurin, but this is expected to have a negligible influence on the spectrum, since the Cu−O bond is so long that the interaction is very weak.[7]

TABLE 3: Calculated Excitation Energies, Oscillator Strengths, and Spin Populations of the Various States of $Co(Im)_2(SH)(SH_2)(HCONH_2)^+$

	spin populations[a]							
	Co		S_{cys}		excitation energy		exptl spectrum	
state	$3d_\sigma$	$3d_\pi$	$3p_\sigma$	$3p_\pi$	(cm^{-1})	osc. strength	of Co−azurin[b]	assignment
X^4A''	1.91	0.95	0.04	0.02				
b^4A''	1.95	0.94	0.01	0.02	3 483	0.00001		LF
a^4A'	0.95	1.92	0.03	0.03	4 079	0.00000		LF
b^4A'	2.12	0.78	0.03	0.01	4 517	0.00000		LF
c^4A''	1.96	0.96	0.01	0.02	6 703	0.00010		LF
c^4A'	1.25	1.68	0.01	0.02	7 315	0.00001		LF
d^4A''	1.91	0.99	0.04	0.00	9 693	0.00007		LF
d^4A'	1.53	1.33	0.04	0.03	15 766	0.00015	15 500 sh	LF
e^4A''	1.90	0.96	0.05	0.02	16 864	0.00051	15 670 (490)	LF
							19 050 sh	
f^4A''	1.92	0.97	0.03	0.01	20 864	0.00049	19 160 (200)	LF
e^4A'	1.01	0.98	0.03	0.95	25 865	0.00098	24 700 sh	CT $\pi S_{cys} \rightarrow Co$
g^4A''	1.25	0.89	0.42	0.34	25 883	0.00060		CT $\sigma\pi S_{cys} \rightarrow Co$
h^4A''	0.38	1.61	0.17	0.79	28 444	0.00135	26 700 (1180)	CT $\pi S_{cys} \rightarrow Co$
f^4A'	0.83	0.96	0.51	0.63	28 596	0.00021		CT $\sigma\pi S_{cys} \rightarrow Co$
g^4A'	1.83	0.14	0.86	0.07	32 741	0.00199	30 300 (3020)	CT $\sigma S_{cys} \rightarrow Co$
i^4A''	1.09	0.97	0.80	0.03	33 280	0.00160		CT $\sigma S_{cys} \rightarrow Co$

[a] Co $3d_\sigma = 3d_{x^2-y^2} + 3d_{z^2} + 3d_{xz}$, Co $3d_\pi = 3d_{xy} + 3d_{yz}$, S_{cys} $3p_\sigma = 3p_x + 3p_z$, S_{cys} $3p_\pi = 3p_y$. [b] The molar absorbance (M^{-1} cm^{-1}) is given in parentheses; sh = shoulder.[32]

TABLE 4: Calculated Excitation Energies, Oscillator Strengths, and Spin Populations of the Various States of $Cu(Im)_2(SH)(SH_2)^+$

	spin populations[a]							
	Cu		S_{cys}		excitation energy		exptl spectrum	
state	$3d_\sigma$	$3d_\pi$	$3p_\sigma$	$3p_\pi$	(cm^{-1})	osc. strength	of plastocyanin[b]	assignment
X^2A''	0.00	0.17	0.00	0.83				
a^2A'	0.34	0.00	0.54	0.00	5 237	0.00001	5 000	LF
b^2A'	0.90	0.00	0.03	0.00	13 330	0.00002	10 800(0.0031)	LF
b^2A''	0.00	0.89	0.00	0.09	14 776	0.00340	12 800(0.0114)	LF
c^2A'	0.99	0.00	0.00	0.00	14 636	0.00001	13 950(0.0043)	LF
c^2A''	0.00	0.86	0.00	0.12	15 403	0.13446	16 700(0.0496)	CT $\pi S_{cys} \rightarrow Cu$
d^2A'	0.75	0.00	0.20	0.00	21 506	0.00074	21 390(0.0035)	CT $\sigma S_{cys} \rightarrow Cu$

[a] Cu $3d_\sigma = 3d_{x^2-y^2} + 3d_{z^2} + 3d_{xz}$, Cu $3d_\pi = 3d_{xy} + 3d_{yz}$, S_{cys} $3p_\sigma = 3p_x + 3p_z$, S_{cys} $3p_\pi = 3p_y$. [b] Experimental oscillator strengths are given in parentheses.[3]

This is confirmed by the experimental absorbance and MCD spectra of *Alcaligenes denitrificans* azurin, which are closely similar to those of plastocyanin.[31]

Tables 3 and 4 show the calculated excitation energies and oscillator strengths of the various ligand-field and charge-transfer states studied in the investigation of the Co(II) and Cu(II) models. To characterize the various excited states, we used the (Mulliken) spin populations, describing the distribution of the one or three unpaired electrons in the Cu(II) and Co(II) models, respectively. In all cases, virtually all spin density is found either in the metal 3d orbitals or in the S_{cys} 3p orbitals. The remaining contributions, from the imidazoles or the axial ligands, constitute less than about 0.1 electrons and remain more or less constant for the various states. They are therefore not included in the tables. The spin populations in the Co/Cu 3d and S_{cys} 3p orbitals are further divided into σ and π parts, to help identify the different charge-transfer states.

Free Co^{2+} has a ^4F ground state, with a second quartet state, ^4P, lying at 14 561 cm^{-1}. As such, ten spin-allowed ligand-field states are expected to appear in the electronic spectrum of Co-substituted azurin, as opposed to only five (originating from Cu^{2+} ^2D) in the native protein. Furthermore, with three holes in the cobalt 3d shell, excitations originating from S_{cys} $3p_\sigma$ and S_{cys} $3p_\pi$ may give rise to six charge-transfer states, as opposed to only two in the native protein. As can be seen from Table 3 the three groups of excitations appear at well-separated energies in the cobalt spectrum. The Co(II) ^4F ground state is split by the ligand field into seven states, found at excitation energies below 10 000 cm^{-1}. The three ^4P states are calculated at 5 000−10 000 cm^{-1} higher energies. The ^4P states have significantly higher calculated oscillator strengths than the ^4F states. They can therefore be expected to be observed in the absorption spectrum, and indeed four weak bands are found in the experimental spectrum in the 15 000−20 000 cm^{-1} region.[32] The two lowest bands can be assigned to the transitions to the d $^4A'$ and e $^4A''$ states on the basis of the excitation energies, while the two bands around 19 000 cm^{-1} should be assigned to the f $^4A''$ state, which is probably split into two by spin-orbit coupling. It is notable that the spin populations in Table 3 clearly show that for the ten lowest states in the spectrum, the three unpaired electrons are almost entirely located in the Co 3d orbitals. This confirms that these are genuine ligand-field states.

Well-separated from the ligand-field states, we find the six charge-transfer states (between 25 000 and 34 000 cm^{-1}), with one unpaired electron located in the S_{cys} 3p orbitals. Experimental studies of the spectrum of Co−azurin have reported at most three charge-transfer bands.[32−35] This is explained by the calculated results in Table 3, showing that the six charge-transfer excitations appear in three pairs of close-lying states. The first two pairs both contain one state corresponding to one S_{cys} $3p_\pi \rightarrow$ Co excitation and one state containing a mixture of S_{cys} $3p_\sigma \rightarrow$ Co and S_{cys} $3p_\pi \rightarrow$ Co excitations, whereas the third pair consists of two excitations out of the S_{cys} $3p_\sigma$ orbital. In the first two pairs, the highest oscillator strength is calculated for

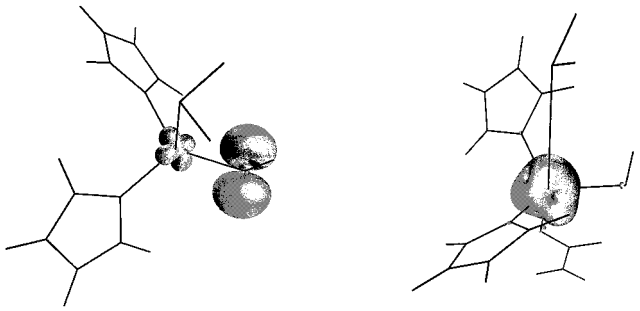

A B

Figure 4. Calculated spin density of the ground state of the $Cu(Im)_2(SH)(SH_2)^+$ (A) and $Co(Im)_2(SH)(SH_2)(HCONH_2)^+$ (B) models.

the S_{cys} $3p_\pi \rightarrow$ Co excitation, and the lowest two charge-transfer bands in the experimental spectrum are therefore assigned to these excitations. This assignment predicts that the intensity of the charge-transfer bands should increase with the energy, which agrees with the experiments. Actually, the calculated oscillator strength of the first S_{cys} $3p_\pi \rightarrow$ Co excitation, 0.00098, is rather low for a charge-transfer transition. Therefore, the corresponding band at 24 700 cm^{-1} is only a shoulder in the experimental spectrum. This band has been observed in all experimental studies of the Co−azurin spectrum, but it has received a varying assignment; it has been attributed to a $S_{met} \rightarrow$ Co transition,[35] to a S_{cys} $3p_\pi \rightarrow$ Co transition,[34] to a cytochrome impurity,[33] or it has been left unassigned.[32] Our calculations confirm the second suggestion. The two more intense bands in the spectrum have been assigned as $S_{cys} \rightarrow$ Co transitions in all previous studies, although the distinction between S_{cys} $3p_\pi$ and S_{cys} $3p_\sigma$ was not always made.

3.3 Comparison of the Co−S_{cys} and Cu−S_{cys} Bonds. Table 4 shows the results obtained for the spectrum of the Cu(II) model. These results are taken from our previous study on the plastocyanin spectrum,[4] where they were discussed in detail. They are included for comparison with the Co(II) spectrum. Apart from the larger number of states appearing in the latter spectrum, there are some major differences in the spectra of the two ions, which can be brought back to the differing electronic structure of the ground state in the two metals. This can be seen from a comparison of the calculated ground state spin density, shown in Figure 4, and from the corresponding spin populations in Tables 3 and 4. The spin density of the Cu(II) model is typical for an axial type 1 copper protein with a trigonal structure, where the singly occupied orbital is strongly delocalized over the Cu $3d_\pi$ and S_{cys} $3p_\pi$ orbitals. In fact, the spin populations in Table 4 indicate that the spin density in the S_{cys} $3p_\pi$ orbital is higher than in the Cu $3d_\pi$ orbital. Even in the first excited state, the $^2A'$ state, which is characterized by a singly occupied Cu−$S_{cys}\sigma$ orbital, the spin density is strongly delocalized over the Cu−S_{cys} bond. Both spin densities are indicative of a strongly covalent Cu−S_{cys} bond. Actually, as we have seen in a previous study,[16] the covalent character of the Cu−S_{cys} bond is the most important factor determining the structure of the active site in azurin and other blue copper proteins: trigonal (with a Cu−S_{cys} π bond) or tetragonal (with a Cu−S_{cys} σ bond), but always much closer to a tetrahedron than the preferred square planar structure of most inorganic, and more ionic, Cu(II) complexes.

On the other hand, the Co(II) model does not show any sign of a strong delocalization of the unpaired electrons. Instead, 95% of the spin density is located in the Co(II) 3d orbitals, with a small and almost equal contribution from S_{cys} (2%), the two imidazole nitrogens (1% each), and the backbone oxygen (1%) (no spin density is found on the methionine model). This indicates that Co(II) forms ionic bonds with all four coordinating ligands, including S_{cys}. Figure 4 also shows that the shape of the spin density is almost perfectly cubic, as it would be in a perfect tetrahedron, the preferred geometry of most four-coordinate inorganic Co(II) complexes, with a nondegenerate $e^4t_2^3$ $^4A_1$ ground state and therefore no driving force for a Jahn−Teller distortion. This gives further support to the observation in the previous section that the preferred (and observed) coordination environment of Co(II) in azurin is a (distorted) tetrahedron.

The difference between the ground-state electronic structure of the two transition metal ions is also responsible for the difference in position and intensity of the charge-transfer bands in the electronic spectra of the two proteins. The soft Cu−S_{cys} bond in the native protein is responsible for the appearance of low-lying $S_{cys} \rightarrow$ Cu charge-transfer excitations: the states c $^2A''$ and d $^2A'$. The former involves an excitation from the Cu−S_{cys} π bonding to the corresponding antibonding molecular orbital. The large overlap between the two orbitals is responsible for the high intensity of this transition and the intense blue color of the protein. The second charge-transfer state (d $^2A'$) involves a $\sigma \rightarrow \pi$ excitation. The orbitals involved are orthogonal in the trigonal (C_s) structure of azurin, and this excitation has therefore little intensity (but gains intensity in the tetragonal type 1 proteins[5]). On the other hand, the ionic Co−S_{cys} interaction in Co−azurin indicates that the Co(II) ion is much more resistant to reduction. The $S_{cys} \rightarrow$ Co excitations are therefore shifted to a considerably higher energy. Moreover, since the orbitals involved are localized on either S_{cys} or Co, all charge-transfer excitations are necessarily rather weak. On the whole, the electronic spectrum of Co−azurin resembles much more the spectra observed for simple inorganic Co(II) complexes than the Cu(II) spectrum.

4 Concluding Remarks

We have presented a detailed investigation of the geometric and electronic structure of Co(II)-substituted azurin and compared it with corresponding results for the native copper protein. For the spectra calculations, Co(II) with three unpaired electrons is more demanding than Cu(II) with only one unpaired electron. Thus, the spectrum consists of nine ligand-field transitions compared to four for Cu(II), and there are six rather than two charge-transfer transitions involving S_{cys}. This has forced us to use less accurate methods than in our previous studies of the spectra of blue copper proteins.[4,5,15] Thus, we have used a model enforced to be of C_s symmetry and without any methyl groups on the cysteine, methionine, and backbone models. Moreover, we have not included any model of the surrounding protein and solvent. In our previous study of the spectrum of plastocyanin we have shown that several of these omissions may quite strongly influence the position of the excited states.[4] However, these errors partly cancel out, so that in the case of plastocyanin qualitatively correct results were obtained for the spectrum already when a symmetric $Cu(Im)_2(SH)(SH_2)^+$ model was used, closely similar to the one used in the present investigation. Therefore, it is not too surprising that we have been able to assign the spectrum of Co−azurin with an error less than 2500 cm^{-1}, i.e., within the normal error limits of the CASPT2 method.[22]

More importantly, we have explained the differences in the geometry and the spectra between Co(II) and Cu(II). These can be related to the electronic structure of the two ions. Co(II) forms much more ionic bonds with S_{cys} than Cu(II), which explains

why the charge-transfer transitions in Co−azurin are weaker and occur at higher energies than in the native protein. Moreover, Cu(II) forms a strong π bond with S_{cys} in native azurin, which makes the bonds to the axial methionine and backbone amide ligands very weak and flexible. This gives rise to the trigonal bipyramidal active site in this protein, and it explains why the bonds to the axial ligands are mainly determined by interactions with the protein. Co(II) on the other hand forms a rather strong bond to the backbone amide group as well as S_{cys} and the imidazole ligands, giving rise to a tetrahedral coordination geometry. The interaction with the methionine ligand, on the other hand, is approximately as weak as in the native protein, and again the Co−S_{met} bond length is mainly determined by the protein.

Altogether, we have once again[30] shown that the geometry and the properties of the blue copper proteins are determined by the preferences of the metal ion and its ligand. The protein has only a small influence on these properties, corresponding to an energy less than 6 kJ/mole. Moreover, this influence originates mainly from hydrogen bonds, nonpolar interactions, and solvation effects, whereas mechanical strain is of minor significance.

Acknowledgment. This investigation has been supported by grants from the Flemish Science Foundation (FWO), the Flemish Government (GOA), the Swedish Natural Science Research Council (NFR), and the European Commission through the TMR program (grant ERBFM-RXCT960079). This work was also supported with computing resources by the Leuvens Universitair Dienstencentrum voor Informatica en Telematica (LUDIT), Leuven, the Swedish Council for Planning and Coordination of Research (FRN), and Parallelldatorcentrum (PDC) at the Royal Institute of Technology in Stockholm.

References and Notes

(1) Sykes, A. G. *Adv. Inorg. Chem.* **1990**, *36*, 377.
(2) Adman, E. T. *Adv. Protein Chem.* **1991**, *42*, 145.
(3) Gewirth, A. A.; Solomon, E. I. *J. Am. Chem. Soc.* **1988**, *110*, 3811.
(4) Pierloot, K.; De Kerpel, J. O. A.; Ryde, U.; Roos, B. O. *J. Am. Chem. Soc.* **1997**, *119*, 218.
(5) Pierloot, K.; De Kerpel, J. O. A.; Ryde, U.; Olsson, M. H. M.; Roos, B. O. *J. Am. Chem. Soc.* **1998**, *120*, 13156.
(6) Ryde, U.; Olsson, M. H. M.; Roos, B. O.; Pierloot, K.; De Kerpel, J. O. A. *Encycl. Comp. Chem.* **1998**, *3*, 2255.
(7) Lowery, M. D.; Solomon, E. I. *Inorg. Chim. Acta* **1992**, *233*, 198.
(8) Bertini, I.; Luchinat, C. *NMR of Paramagnetic Molecules in Biological Systems*; The Benjamin/Cummings Publishing Company: New York, 1986.
(9) Bertini, I.; Turano, P.; Vila, A. *Chem. Rev.* **1993**, *93*, 2833.
(10) Bertini, I.; Luchinat, C. In *Advances in Bioinorganic Chemistry*; Eichorn, G. L., Marzilli, L. G., Eds.; Elsevier: New York, 1984; pp 72−111.
(11) Baker, E. N. *J. Mol. Biol.* **1988**, *203*, 1071.
(12) Moratal, J. M.; Romero, A.; Perales-Alarcón, A.; Jimenez, H. R. *Eur. J. Biochem.* **1995**, *102*, 4360.
(13) Bonander, N.; Vänngård, T.; Tsai, L.-C.; Nar, V. L. H.; Sjölin, L. *Proteins: Struc. Funct. Genet.* **1997**, *27*, 385.
(14) Ryde, U.; Olsson, M. H. M.; Pierloot, K.; Roos, B. O. *J. Mol. Biol.* **1996**, *261*, 586.
(15) De Kerpel, J. O. A.; Pierloot, K.; Ryde, U.; Roos, B. O. *J. Phys. Chem. B* **1998**, *102*, 4638.
(16) Olsson, M. H. M.; Ryde, U.; Roos, B. O.; Pierloot, K. *J. Biol. Inorg. Chem.* **1998**, *3*, 109.
(17) Olsson, M. H. M.; Ryde, U.; Roos, B. O. *Protein Sci.* **1998**, *7*, 2659.
(18) Williams, R. J. P. In *Molecular Basis of Enzyme Action and Inhibition*; Desnuelle, P. A. E., Ed.; Pergamon Press: Oxford, 1963; pp 133−149.
(19) Malmström, B. G. In *Oxidases and Related Redox Systems*; King, T. E., Mason, H. S., Morrison, M., Eds.; J. Wiley & Sons: New York, 1965; pp 207−216.
(20) Ahlrichs, R.; Bär, M.; Baron, H.-P.; Bauernschmitt, R.; Böcker, S.; Ehrig, M.; Eicjkorn, K.; Elliott, S.; Haase, F.; Häser, M.; Horn, H.; Huber, C.; Kölmel, C.; Kollwitz, M.; Ochsenfeld, C.; Öhm, H.; Schäfer, A.; Schneider, U.; Treutler, O.; von Arnim, M.; Weigend, F.; Weis, P.; Weiss, H. *TURBOMOLE Version 4.5*, Universität Karlsruhe, Germany, 1997.
(21) Schäfer, A.; Horn, H.; Ahlrichs, R. *J. Chem. Phys.* **1992**, *97*, 2571.
(22) Roos, B. O.; Andersson, K.; Fülscher, M. P.; Malmqvist, P.-Å.; Serrano-Andrés, L.; Pierloot, K.; Merchán, M. In *Advances in Chemical Physics: New Methods in Computational Quantum Mechanics*; Prigogine, I., Rice, S. A., Eds.; John Wiley & Sons: New York, 1996; Vol XCIII, pp 219−331.
(23) Pierloot, K.; Dumez, B.; Widmark, P.-O.; Roos, B. O. *Theor. Chim. Acta* **1995**, *90*, 87.
(24) Roos, B. O.; Andersson, K.; Fülscher, M. P.; Serrano-Andrés, L.; Pierloot, K.; Merchán, M.; Molina, V. *J. Mol. Struct. (Theochem)* **1996**, *388*, 257.
(25) Malmqvist, P. Å.; Roos, B. O. *Chem. Phys. Lett.* **1989**, *155*, 189.
(26) Andersson, K.; Blomberg, M. R. A.; Fülscher, M. P.; Karlström, G.; Lindh, R.; Malmqvist, P.-Å.; Neogrády, P.; Olsen, J.; Roos, B. O.; Sadlej, A. J.; Schütz, M.; Seijo, L.; Serrano-Andrés, L.; Siegbahn, P. E. M.; Widmark, P.-O. *MOLCAS Version 4*, Lund University, Sweden, 1997.
(27) Nar, H.; Messerschmidt, A.; Huber, R.; van de Kamp, M.; Canters, G. W. *J. Mol. Biol.* **1991**, *218*, 427.
(28) Olsson, M. H. M.; Ryde, U.; Roos, B. O. Theoretical study of the copper coordination sphere of azurin. To be published.
(29) De Kerpel, J. O. A.; Ryde, U. Protein strain in blue copper proteins studied by free energy perturbations. Proteins: Struct., Funct., Genet. **1999**, *36*, 157.
(30) Ryde, U.; Olsson, M. H. M.; Roos, B. O.; Kerpel, J. O. A. D.; Pierloot, K. On the role of strain in blue copper proteins. *J. Biol. Inorg. Chem.*, invited commentary, 1999.
(31) LaCroix, L. B.; Randall, D. W.; Nersissian, A. M.; Hoitink, C. W. G.; Canters, G. W.; Valentine, J. S.; Solomon, E. I. *J. Am. Chem. Soc.* **1998**, *120*, 9621.
(32) Di Bilio, A. J.; Chang, T. K.; Malmström, B. G.; Gray, H. B.; Karlsson, B. G.; Nordling, M.; Lundberg, L. G. *Inorg. Chim. Acta* **1992**, *198*, 145.
(33) McMillin, D. R.; Rosenberg, R. C.; Gray, H. B. *Proc. Nat. Acad. Sci.* **1974**, *71*, 4760.
(34) Tennent, D. L.; McMillin, D. R. *J. Am. Chem. Soc.* **1979**, *101*, 2307.
(35) Maritano, S.; Marchesini, A.; Suzuki, S. *J. Biol. Inorg. Chem.* **1997**, *2*, 177.